

Water Absorption Characteristics of Hybrid Materials Incorporating Tetrabutyl Titanate with Acrylic Polymer Via Sol–Gel Process

F. X. Perrin, V. N. Nguyen, J. L. Vernet

Laboratoire de Chimie Appliquée, Université de Toulon et du Var, BP132, 83957 La Garde Cedex, France

Received 16 February 2004; accepted 22 November 2004

DOI 10.1002/app.21736

Published online in Wiley InterScience (www.interscience.wiley.com).

ABSTRACT: The sol–gel process was used to prepare organic/inorganic hybrids utilizing a terpolymer of *n*-butyl methacrylate, methyl methacrylate, and methacrylic acid as an organic phase and titanium tetrabutoxide as a precursor of the inorganic phase. Such hybrid materials may be of interest as primers for corrosion protection of metal substrates. In the absence of electrochemical influence, which is usually provided by anticorrosive pigments in current protective coatings, the barrier mechanism becomes one of the basic elements for protecting metals against atmospheric corrosion. In that context, we report the water uptake characteristics of hybrid films with titania content up to 16.3 wt

%. The slow hydrolysis of butoxy, acetate, and carboxylate ligands, which becomes more and more obvious with an increase in titanium oxide cluster content, is found to produce a chemically driven force for water uptake in hybrids. The 4.6 wt % TiO₂ hybrid results in the best balance of properties with a far lower diffusion coefficient and nearly the same amount of water absorbed at saturation compared to the polymer matrix. © 2005 Wiley Periodicals, Inc. *J Appl Polym Sci* 97: 92–102, 2005

Key words: nanocomposites; diffusion; IR spectroscopy; water uptake; water structure

INTRODUCTION

Sol–gel processing of organic–inorganic nanocomposites has attracted great interest in the last two decades because the nanostructure offers the opportunity to obtain new materials with tunable properties.^{1–3} Such a nanostructure is obtained when the organic and inorganic components are linked together through either covalent or hydrogen bonds. We previously reported the preparation and mechanical properties of acrylic hybrids with methacrylic acid (MA) units able to react with titanium alkoxide to give COOTi coordinative bonds.^{4,5} Because of the restrictive legislation concerning the use of anticorrosive pigments (mostly based on highly toxic chromates⁶), these hybrids can be potentially interesting as new protective coatings with minimal environmental impact. Monte and Sugerman⁷ prepared “pure” inorganic coatings by the sol–gel process that can only be applied as thin adherence promoter layers for a subsequent organic coating or paint. (Cracking is observed when the thickness exceeds a few microns because of stress generated during network formation and solvent

evaporation.) Our aim was to prepare a coating that on its own can efficiently protect metals from corrosion. That is why the organic–inorganic hybrid approach was adopted. Moreover, contrary to Monte and Sugerman,⁷ we are also interested in the barrier properties of our coatings and especially their water absorption characteristics.

In relation to other binders, acrylic resins offer a number of advantages such as excellent weatherability and high resistance to acidic and alkaline hydrolysis, to discoloration on heating, and even to oxidizing environments.⁸ The high ratio of the soft *n*-butyl methacrylate (BMA; glass-transition temperature of the homopolymer +20°C) in poly(methyl methacrylate-*co*-BMA-*co*-MA) [P(MMA-*co*-BMA-*co*-MA), 0.16/0.80/0.04; Elvacite 2550, Ineos Acrylics] offers interesting properties in regard to protective coatings applications, such as flexibility (and thus resistance to stress cracking) and hydrophobicity (and thus low permeability, giving effective protection through the barrier mechanism⁹). The adhesion of this polymer to metal substrates can possibly be improved by incorporating a ceramic titania phase that can form chemical bonds at the interface with reactive groups at the surface of the oxide layer.⁷

A direct way to impart resistance to water disbondment (wet adhesion) is to prevent the access of water by using a very small permeability, thick system. In the development of such hybrid coatings where the

Correspondence to: F. X. Perrin (francois-xavier.perrin@univ-tln.fr).

Contract grant sponsor: Egide.

passivation mechanism by anticorrosive pigments or corrosion inhibitors is not operative, it is therefore necessary to optimize their permeability for water. Thus far, thermodynamic and kinetic studies concerning water uptake of nanocomposites involving the *in situ* generation of inorganic nanoparticles through the sol-gel process are rather scarce and mostly limited to hydrophilic organic components [e.g., poly(phenylene terephthalamide),¹⁰ poly(trimethylhexamethylene terephthalamide),¹¹ poly(2-hydroxyethyl acrylate-co-methyl acrylate),¹² and polyimide¹³]. Although Shantali et al. recently found enhanced water solubility and diffusivity in polyimide/SiO₂ hybrids compared to the polyimide matrix,¹³ opposite trends are usually reported and ascribed either to the denser molecular packing and lower mobility of the inorganic phase¹² or to the engagement of the polar groups from the polymer through secondary bonds with the *in situ* generated silica¹¹ or titania.¹⁰

It is the aim of this study to investigate the water uptake characteristics of hybrids prepared from a relatively hydrophobic P(MMA-co-BMA-co-MA) polymer matrix and titanium tetrabutoxide. Apart from the extraction of solubility and diffusion coefficients from the gravimetric data, thermogravimetric analysis (TGA) and FTIR spectroscopy have also been performed to better understand the effect of the oxo-clusters on the state of sorbed water in hybrids.

EXPERIMENTAL

Preparation of hybrids

Hybrid organic-inorganic materials based on an MMA (16 mol %)-BMA (80 mol %)-MA (4 mol %) terpolymer (AP, Ineos Acrylics) have been prepared by the *in situ* sol-gel process in the presence of titanium tetrabutoxide [Ti(OBu)₄, 97%, Aldrich] as described elsewhere.⁵ The whole hydrolysis-condensation process results in homogeneous and semitransparent films. Note that the inorganic component will often be referred to in this article as TiO₂ or titania, even though, strictly speaking, there is no titania in our hybrids but rather partially uncondensed titanium oxide clusters.¹⁴ In this work, and contrary to the previous microhardness study,⁵ the sol synthesis route includes or does not include acetic acid as an organic acid modifier. These specific experimental conditions are mainly commanded by applicability considerations and protective properties (details not shown). The composition of the investigated sols is shown in Table I. Apart from the samples shown in Table I, additional composites were prepared from a P(MMA-co-BMA) copolymer (Ineos Acrylics) with 89 mol % MMA and 11 mol % BMA following the same procedure.

For gravimetric measurements, the sols were poured into a Teflon mold and successively cured for

TABLE I
Composition of Hybrids

Sample code	(Ti)/(COOH) ^a molar ratio	TiO ₂		Chelating agent (acetic acid)
		wt % ^b	vol % ^c	
AP	0	0	0	No
AP-2	2	4.6	2.3	Yes ^d
AP-4	4	8.8	4.6	Yes ^d
AP-6	6	12.7	6.8	No
AP-8	8	16.3	8.8	No

All samples are prepared with non-prehydrolyzed sols.

^a Carboxylic groups from the polymer.

^b Calculated percentage assuming 100% conversion of metal alkoxide to TiO₂ and totally removed acetic acid.

^c Calculated from the relationship $\text{vol \%} = \text{wt \%} \times d_{\text{hybrid}}/d_{\text{titania}}$ where wt % is the weight percent of titania content, d_{hybrid} is the density of the hybrid material, and d_{titania} is the density of the pure sol-gel titania.

^d Acetic acid (AcOH) is added to give a molar ratio of AcOH/Ti = 3.

5 days at room temperature under a nearly constant 60% relative humidity and under a vacuum for 1 day at 80°C to give 500- μm free films. Before beginning the sorption tests, each sample was further stored for 1 month in a desiccator because changes in the properties that are partly due to physical aging were found to be significant during this period of time.⁵

Characterization methods

For the gravimetric method, the free films were immersed in distilled water at 24°C, periodically removed, dried carefully with filter paper, and weighed using a balance OHAUS-Explorer with a precision of 0.1 mg. Three separate measurements were carried out for each sample type, and the experimental results are always included in the size of the data dots.

The thermal analyses were monitored by a DTA-TGA 92-1750 Setaram apparatus. To study the desorption of water, one piece with a given thickness (500 μm) and geometry was systematically cut and placed inside the crucible for analysis. The typical thermal analysis run was carried out under a constant argon flow at a 10°C min⁻¹ heating rate starting from an initial temperature (T_0) of 25°C and ending at 200°C. Each run was repeated at least twice. The thermal effect (heat flow vs. T), TG trace (mass loss vs. T), and its time derivative TG (DTG, milligrams lost water per degree Kelvin) were simultaneously recorded. All DTG traces were normalized to a 1-mg water content at equilibrium.

The heat flow trace allowed us to verify that the broad endothermic peak observed in the investigated temperature range was related to water vaporization, the relevant enthalpies being rather close to 2.3 kJ g⁻¹,

the vaporization enthalpy of pure water in this temperature range.

Attenuated total reflectance (ATR)-FTIR spectra were recorded on a Nexus Nicolet spectrometer. The ATR accessory (Thunderdome ATR monoreflexion system) contained a germanium internal reflection element (IRE) at a nominal incident angle of 45° and yielding only one reflection at the sample surface. All spectra (64 scans at 4 cm⁻¹ resolution) were recorded at 302 K.

The incident radiation's depth of penetration (d_p) is defined as the distance required for the electric field amplitude to fall to e^{-1} of its value at the surface. It is given by

$$d_p = \frac{\lambda/n_1}{\left[2\pi\left(\sin^2\theta - \left(\frac{n_2}{n_1}\right)^2\right)\right]^{1/2}}$$

where λ is the wavelength of the incident radiation, θ is the incident angle of the IR beam, n_1 is the refractive index of the IRE, and n_2 is the refractive index of the polymer. In the region of the water stretching bands (i.e., $\lambda \approx 2.86 \mu\text{m}$) and because $n_1 = 4$, $n_2 \approx 1.5$, and $\theta = 45^\circ$, the d_p value is about 0.48 μm .

For IR analysis, $\approx 200 \mu\text{m}$ thick films with no visible defects (cracks, bubbles, etc.) were immersed in liquid water for 96 h, removed from the water, cautiously blotted with clean filter paper to totally remove the water on top of the film, and clamped to the IRE surface for spectra recording. The total removal of water on top of the film ensures that the IR beam only probes the water in the film.

Elemental analysis was performed by the Service Central d'Analyse of CNRS (Vernaison, France).

To study the morphology of the prepared composites, free films were cryogenically broken after immersion in liquid nitrogen and the fractured surfaces were observed by scanning electron microscopy (SEM). To avoid degradation of the sample by the electron beam, the fractured surface was coated with a thin layer of gold before analysis. SEM analysis was carried out with a Phillips XL30 microscope with an EDAX X-ray probe at an accelerating voltage of 15 kV.

RESULTS AND DISCUSSION

Effect of MA units on morphology of acrylate/TiO₂ hybrids

The Soxhlet extraction results in tetrahydrofuran⁴ showed that the percentage of crosslinked polymer approaches zero in composites based on P(MMA-co-BMA) but it can be as high as 73% with P(MMA-co-BMA-co-MA) as the organic matrix. This can be related to the formation of COOTi coordinative bonds in the presence of MA units between the polymer and the

mineral component. Further, the effect of these MA units on the morphology of acrylate/TiO₂ hybrids was investigated using SEM methods. Figure 1 depicts the SEM micrographs of the fracture surface of P(MMA-co-BMA)/TiO₂ and P(MMA-co-BMA-co-MA)/TiO₂ hybrids. In P(MMA-co-BMA)/TiO₂ materials, the aggregates of inorganic particles are uniformly dispersed in the copolymer matrix [Fig. 1(a)]. A higher magnification micrograph (original magnification $\times 8000$) shows that the sizes of the inorganic particles are mostly in the range of 500 nm–1 μm [Fig. 1(b)]. Because some of these particles are larger than the wavelength of visible light, they can cause the scattering of visible light. That is why the P(MMA-co-BMA)/TiO₂ material is optically opaque. The morphology of P(MMA-co-BMA-co-MA)/TiO₂ (4.6–30 wt %) hybrids is clearly different: even with the highest magnification ($\times 31,000$), a co-continuous structure is observed with no macrophase separation. It is noteworthy that the fracture surface becomes rougher with increasing titanium content in P(MMA-co-BMA-co-MA)/TiO₂ hybrids [compare Fig. 1(c,e) at the same magnification]. The above SEM results confirm that the compatibilization in hybrids results from the chemical reaction between —COOH groups of MA units and the titanium alkoxide precursor. Here, the hydrogen bonds formed in the P(MMA-co-BMA)/TiO₂ materials do not impede the macroscopic phase separation.

Mass change measurements

Figure 2 shows the percentage of water uptake for all materials versus the immersion time in distilled water. AP and AP-2 films show an initial high rate of uptake followed by a slower rate, and eventually it reaches equilibrium. Conversely, AP-4 and AP-6 hybrids show a singular behavior with a loss weight observed at the longest immersion times. The time necessary to detect such a weight loss is found to decrease with an increase in titania content in the hybrid material (Table II). Moreover, the weight loss for AP-4 is insignificant compared to the extensive weight loss measured with AP-6.

The amount of carbon and titanium leached out in 50 mL of water were determined by elemental analysis after 0-h (blank), 2-day, and 20-day immersion times for AP-4 and AP-6 films. The titanium concentration is systematically less than 1 $\mu\text{g/L}$ (limit of sensitivity), giving a titanium content of $<0.05 \mu\text{g}$, which is negligible compared to the measured weight losses of close to 100 and 600 μg observed for AP-4 and AP-6 films, respectively, after 20-day immersion.

Conversely, a carbon element is clearly detected and it accounts for 30–60% of the measured film weight loss for AP-4 and AP-6 samples. The above results show that only organic moieties are released into water. Because the weight loss increases with the titania

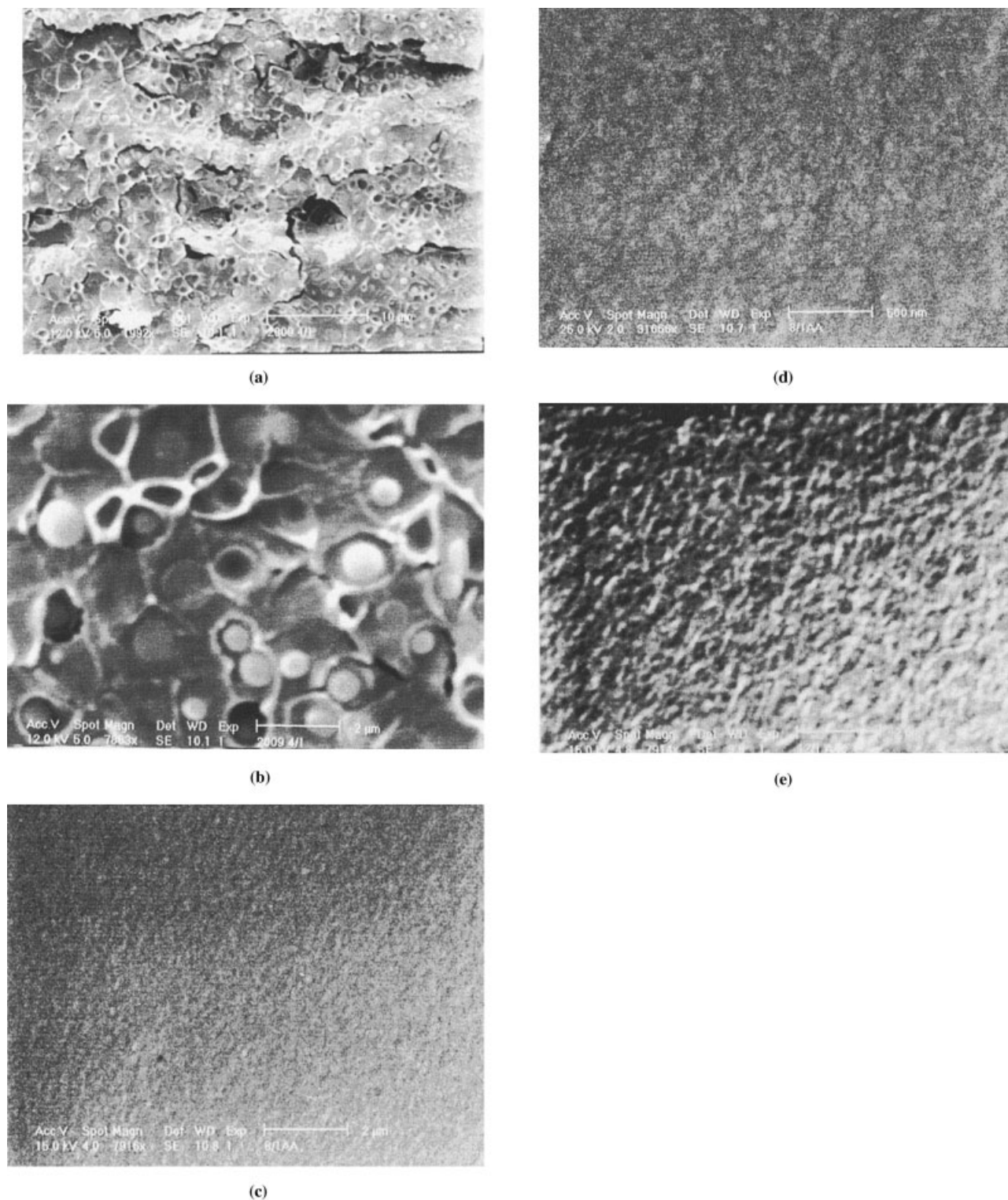


Figure 1 Scanning electron micrographs of (a) P(MMA-*co*-BMA)/TiO₂ (8.8 wt %), (b) P(MMA-*co*-BMA)/TiO₂ (8.8 wt %) at a higher magnification, (c) P(MMA-*co*-BMA-*co*-MA)/TiO₂ (8.8 wt %) (AP-4), (d) P(MMA-*co*-BMA-*co*-MA)/TiO₂ (8.8 wt %) (AP-4) at a higher magnification, and (e) P(MMA-*co*-BMA-*co*-MA)/TiO₂ (30 wt %).

content in the hybrids, we believe that a large part of the released organic compounds comes from the slow hydrolysis of the residual TiOBu groups (mostly bridging butoxy groups that are still present in the

structure of the final hybrid¹⁴) and/or TiOAc groups that are likely promoted by the plasticizing effect of the initially entering water molecules. It must be emphasized that the hydrolysis of COOTi and BuOTi

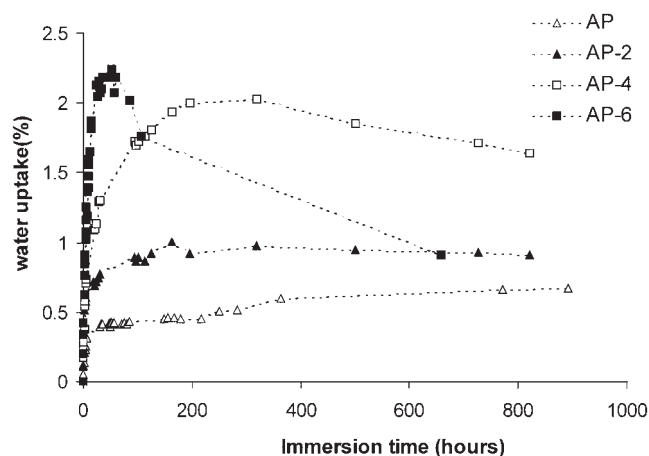
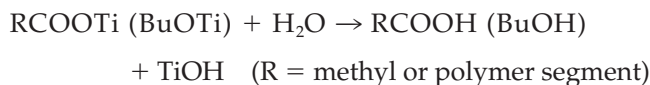


Figure 2 Plots of water uptake (wt %) versus immersion time in water for the acrylic terpolymer and organic/inorganic hybrids.

bonds is a slow process: after 2 days of immersion, no leaching can be detected by elemental analysis for the AP-4 and AP-6 samples.

The maximum water uptake appears to increase with the titania content in hybrids, but the water solubility in AP-2 is relatively low and approaches the water solubility in AP. Here, the titania network appears to not be tight enough to limit water absorption in hybrids compared to the acrylic polymer. Because of the leaching out of organics for AP-4 and AP-6, the maximum water uptake is likely underestimated. The water solubility in polymers is often related to the nature and concentration of its hydrophilic sites. Compared to the acrylic polymer, new potential hydrophilic sites in hybrids are Ti—O—C [from Ti(OBu) residual groups], Ti—OAc (only for AP-2 and AP-4), Ti—O—Ti, and TiOH uncondensed groups. Furthermore, strongly hydrophilic carboxylic groups from the polymer are partly substituted by COOTi coordinative bonds in hybrids. Because AP-6, which does not contain TiOAc sites, has the more pronounced moisture affinity, we infer that the concentration of these groups is too low in AP-2 and AP-4 to significantly contribute to the water uptake. At the moment, further discussion can only be speculative. However, we must remind that the hydroxyl groups in TiOH are much more effective hydrophilic sites than the other potential sites. We also believe that the slow hydrolysis of COOTi and residual TiOBu bonds bring a chemically driven force for water uptake:



In either case, the above reaction releases at least one strongly hydrophilic TiOH site. As far as the

COOTi bonds with the acrylic polymer are concerned, two strongly hydrophilic sites (carboxylic and hydroxy groups) remain in the structure. In that case, apart from releasing two strongly hydrophilic sites, the hydrolysis reaction decreases the crosslinking extent between the organic and the inorganic components and thus increases the free space available for further water absorption. The fact that the concentration of COOTi bonds increases with the titania content⁴ supports the last point of view.

Assuming an ideal Fickian process, the sorption data for a plane sheet geometry is represented by the following equation¹⁵:

$$\frac{M_t}{M_s} = 1 - \frac{8}{\pi^2} \sum_{n=0}^{\infty} \frac{1}{(2n+1)^2} \exp\left[-\frac{(2n+1)^2 D \pi^2}{l^2} t\right] \quad (1)$$

where M_t is the amount of absorbed water at time t , M_s is the amount of water absorbed at saturation, l is the thickness of the freestanding specimen, and D is the diffusion coefficient that is considered to be constant over the exposition time.

At sufficiently short times ($M_t/M_s < 0.5$), the ratio is proportional to the square root of the time,

$$\frac{M_t}{M_s} = \frac{4\sqrt{D}}{1\sqrt{\pi}} \sqrt{t} \quad (2)$$

for a freestanding film. Because TiOBu and TiOAc residual groups in AP-4 and AP-6 hybrids slowly hydrolyze (releasing butanol and acetic acid), our gravimetric results cannot be fitted to eq. (1). That is why we used eq. (2), which is valid at short immersion times (thus far away from the equilibrium), to fit our experimental results. Because water absorption goes with a slow release of organics for AP-4 and AP-6, the equilibrium is never attained in such systems and the maximum water uptake was used in eq. (2) instead of the real amount of water absorbed at saturation, which cannot be strictly determined. In the initial

TABLE II
Summary of Gravimetric Data

Samples	Max. water uptake % (weight)	Loss weight time ^a (days)	Diffusion coefficient $D \times 10^9$ (cm ² /s)
AP	0.7	—	13.6
AP-2	1.0	— ^b	6.5
AP-4	1.9	15	6.7
AP-6	2.3	3	8.5

^a The immersion time as soon as a loss weight can be measured.

^b The weight loss of AP-2 samples is barely perceptible ($\Delta W < 0.07\%$) after immersion times exceeding 20 days.

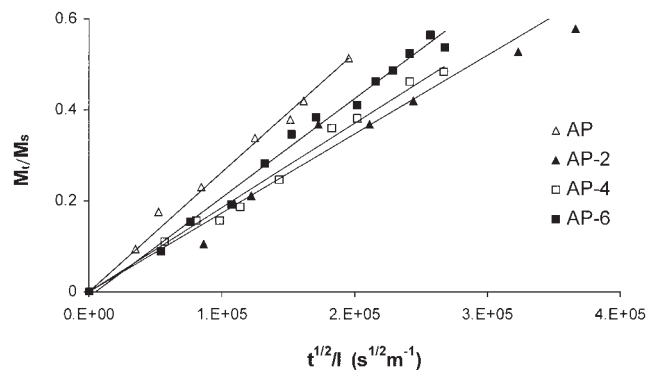


Figure 3 The kinetics of sorption for the acrylic terpolymer and organic/inorganic hybrids. Continuous lines are obtained from the linear regression of the initial points.

times corresponding to fast water uptake, a well-defined linear dependence of the M_t/M_s ratio on $t^{1/2}$ was found (Fig. 3). Because of the simultaneous absorption of water and slow release of organic moieties during the immersion for AP-4 and AP-6, the calculated diffusion coefficients for these hybrids are only the apparent diffusion coefficients. Nevertheless, the variations in D values are sufficiently high to obtain reliable trends concerning the effect of the titanium oxide clusters on the kinetics of water transport. The lower values of D in AP-2, AP-4, and AP-6 than AP may be related to the crosslinked nature of the polymer in the hybrids and the resulting sluggish motion of the polymer chains in relation to each other as revealed before by dynamic mechanical analysis.⁴ A slower sorption kinetics in hybrids can also be ascribed to the stronger specific interactions of water in hybrids (see the new potential hydrophilic sites listed above) compared to the acrylic polymer (mostly ester groups). The slight increase of both D and water uptake when the titania content increases from 4.6 to 12.2 wt % suggests that the effect of this sorption mechanism through specific molecular interactions on the sorption kinetics must not be overestimated. Two more reasonable explanations can be proposed in order to explain the latter D evolution. The first explanation concerns the hydrolysis of COOTi bonds between the polymer and the ceramic phase (more effective in the highest filled hybrids) that results in a less tight and crosslinked molecular structure; a second explanation, although less clear, might be related to the large water clusters that form in higher filled hybrids AP-4 and AP-6 as revealed by FTIR spectroscopy.

The water absorption characteristics (solubility and sorption rate) of the same hybrid materials used as coatings on iron substrates and studied by electrochemical impedance spectroscopy gave the same trends and conclusions as free films (results not shown).

TGA

In a study like this, the more direct results given by TGA obviously concern the measurement of the water uptake by the solid sample. Apart from that, by clarifying the process of water evaporation from an organic or inorganic matrix upon heating, TGA may also offer important information about the chemical structure of solid materials.

Figure 4 reports the TGA traces for the acrylic polymer and hybrids AP-2, AP-4, and AP-6 after immersion in water for 96 h. For all four samples, a continuous weight decrease due to water release can be observed. It must be noted that TGA measures not only water uptake during immersion but also other volatiles (residual toluene and monomers, strongly bound water, and butanol molecules that are formed during the sol-gel process and water absorbed from the atmosphere during the transfer of samples from the desiccator to the TGA apparatus). The first TGA measurements realized were on nonimmersed samples in order to evaluate the initial volatile content of each material (TGA_{0h}). The second TGA measurements were performed on samples after 96-h immersion in water (TGA_{96h}). A relatively low immersion time (96 h) was chosen to minimize the effect of the leaching out of organics for hybrids, as revealed by mass change measurements. Despite that precaution, the difference ($TGA_{96h} - TGA_{0h}$) likely underestimates the actual amount of water uptake. It is easy to relate the TGA measurements to the actual water uptake considering the two borderline cases: the initial volatiles are either totally leached out during the immersion time or not released at all (see Appendix A). The actual water uptake stands between values given by eqs. (A.4) and (A.6) (Table III). The TGA results well agree with mass change measurements except for AP-6. A significant amount of butanol and acetic acid formed during the immersion period are leached out for AP-6. That is why the mass change measurement

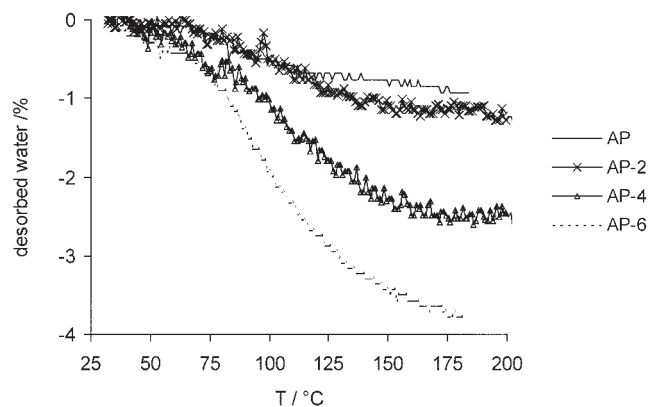


Figure 4 TG curves of AP, AP-2, AP-4, and AP-6 after immersion in water for 96 h.

TABLE III
TGA Measurements on Polymer Matrix and Hybrids and Comparison with Mass Change Measurements

Sample	TGA _{0h} (%)	TGA _{96h} (%)	$\frac{TGA_{th}(100 - TGA_{0h})}{100 - TGA_{th}}$ (%)	$100 \frac{(TGA_{th} - TGA_{0h})}{100 - TGA_{th}}$ (%)
AP	0.23	0.84	0.84	0.61
AP-2	0.27	1.08	1.09	0.82
AP-4	0.91	2.43	2.46	1.55
AP-6	0.90	3.34	3.42	2.53

TGA_{0h}, weight loss of nonimmersed material; TGA_{96h}, weight loss after 96 h of immersion in water.

gives a lower amount of sorbed water compared to TGA.

In addition, Figure 4 shows that the TGA trace reaches a plateau value from a temperature that significantly varies with the investigated sample. For AP, the plateau value starts at about 150°C whereas, for hybrids, weight loss is observed at even higher temperatures: 160, 175, and 180°C for AP-2, AP-4, and AP-6, respectively. This indicates that more tightly bound water is present in the highest filled hybrids (AP-4 and AP-6), thus confirming the FTIR results. This is even clearer from a DTG comparison of the different samples, as shown in Figure 5. The DTG signal appears broader, less intense, and displaced toward high temperatures for AP-4 and AP-6 comparing to AP and AP-2, which reveals a wider distribution of water molecules and the presence of strongly bound water molecules that are more difficult to release for the former materials.

State of water in wet films: FTIR characterization

General observations

The ATR-FTIR spectrum of the sorbed water in the hybrid and acrylic films was obtained by spectral subtraction of the wet film (after immersion for 4 days) from that of the dried film (i.e., film stored for 48 h under a vacuum, 0% relative humidity). All the ATR-FTIR spectra shown in this work are wet-dry difference spectra. The subtraction gives a good approximation of the FTIR spectra of the sorbed water if the residual OH stretching vibrations (residual water and butanol and uncondensed Ti—OH groups) are negligible compared to the sorbed water at equilibrium. This is true in each film investigated, as proved by comparisons of the FTIR spectra of the dried and wet film in the $\nu(\text{OH})$ region (not shown). Otherwise, it is likely that the interaction of sorbed water through hydrogen bonding with the residual —OH groups in

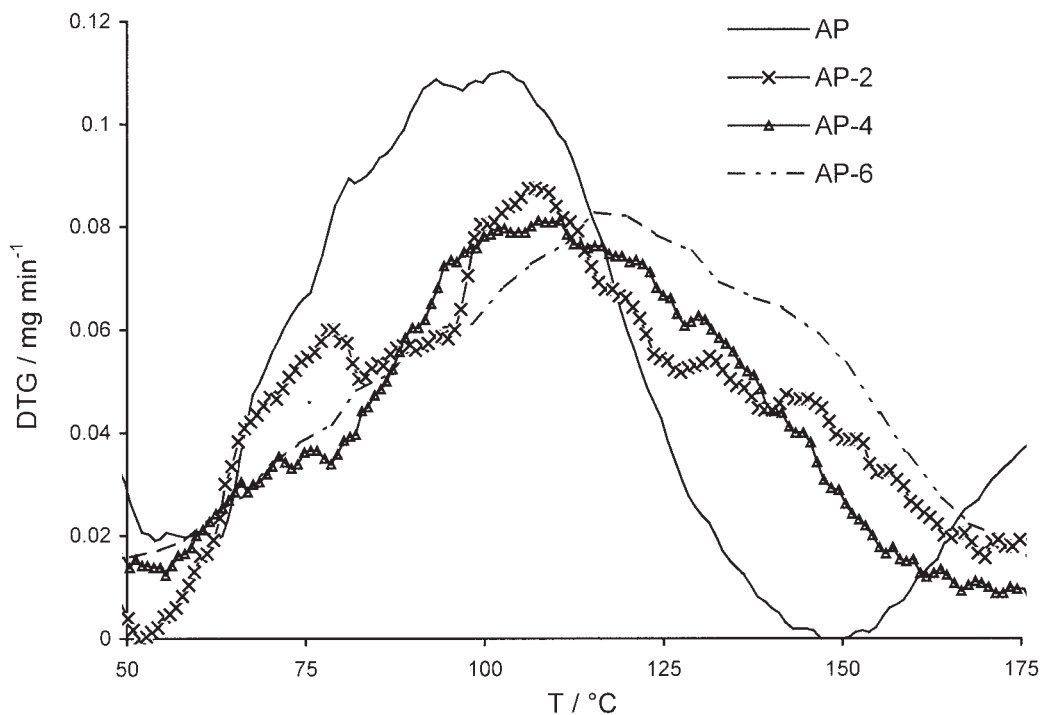


Figure 5 DTG traces of AP, AP-2, AP-4, and AP-6 after immersion in water for 96 h.

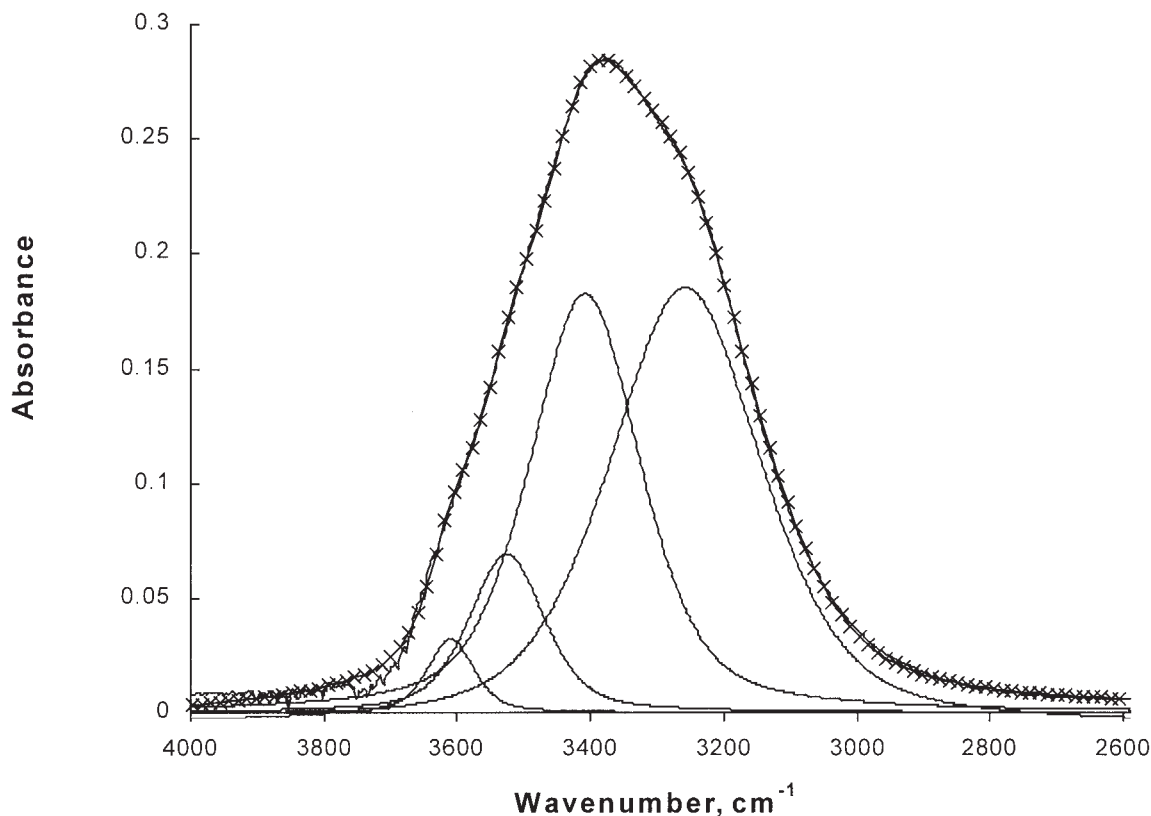


Figure 6 Band fitting results for pure water at 302 K; (-x-) fitted trace.

the dried material would invalidate the spectral subtraction.¹⁶

To quantitatively analyze the amount of sorbed water in polymers using the ATR-FTIR technique, the polymer film must usually be spread, cast, or spun onto the IRE.¹⁷ Here, the transfer of the wet film and wiping of the superficial water before pressure contact with the IRE did not give reproducible results in terms of absolute IR intensities (up to a 20% difference in maximum absorbance was observed for two different pieces of the same wet material). However, as expected from the gravimetric results, the water uptake was found to increase when the titania content increases in hybrid films, particularly when TiO_2 exceeds 8.8 wt %. For lower TiO_2 content, the amount of water absorbed in hybrids is quite comparable with that in the polymer film.

It is more interesting that further insight concerning the state of sorbed water can be inferred from the ATR-FTIR technique by analysis of the change in the band shape of the composite $\nu(\text{OH})$ band. To study the structure of water molecules in hybrid materials, a careful deconvolution of the FTIR spectra in the OH stretching region was carried out for water in P(MMA-BMA-MA) and water in AP-2, AP-4, AP-6, and AP-8 hybrids. Adopting the same strategy as Sammon et al.,¹⁸ a fixed band shape ratio (50% Gaussian/50% Lorentzian) was adopted and all other parameters

were allowed to vary upon iteration. The broad band between 3100 and 3800 cm^{-1} was deconvoluted into four peaks for pure water (Fig. 6), water in P(MMA-BMA-MA) film (Fig. 7), and water in hybrid films (Figs. 8–10). All the reported results gave satisfactory fits with correlation coefficient values > 0.96 . The

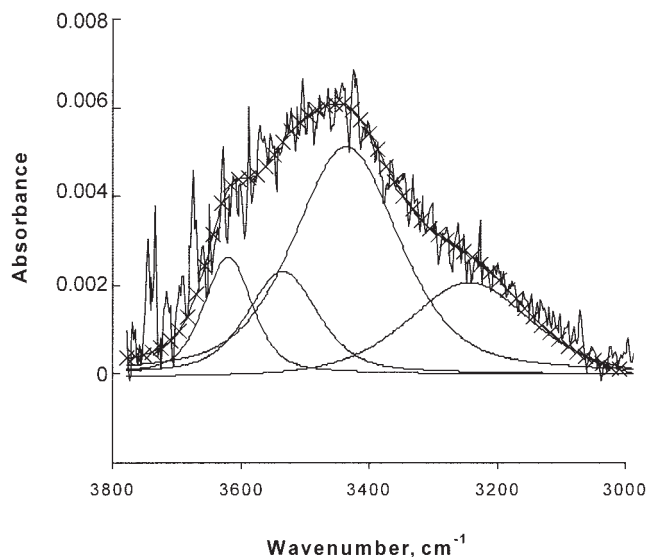


Figure 7 Band fitting results for water in AP; (-x-) fitted trace.

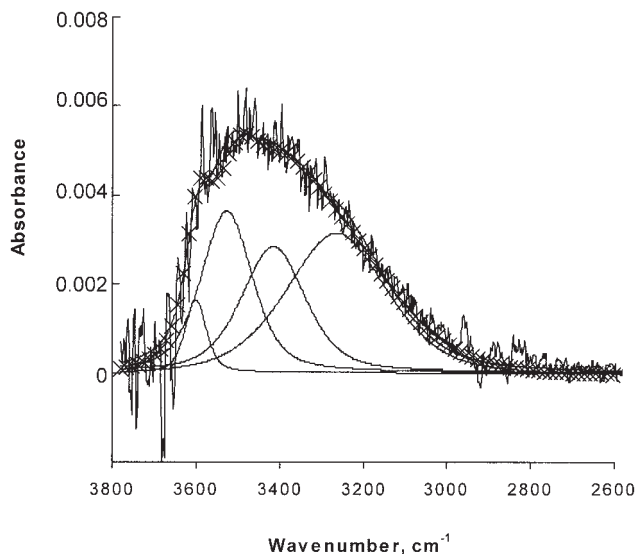


Figure 8 Band fitting results for water in AP-2; (-x-) fitted trace.

curve fit parameters [position, line width (full width at half-maximum), and area] are shown in Tables IV (for bulk liquid water) and V (for water in polymeric films).

For the pure water profile, the frequencies and relative intensities of the four individual peaks are in fairly good agreement with those obtained by Sammon et al.¹⁸ Only a significant positive shift in the frequency of bands 3 and 4 (the latter being more pronounced) can be noted.

Bands 1, 2, and 3 stem from monomeric water (or matrix-isolated dimers), hydrogen-bonded dimers or

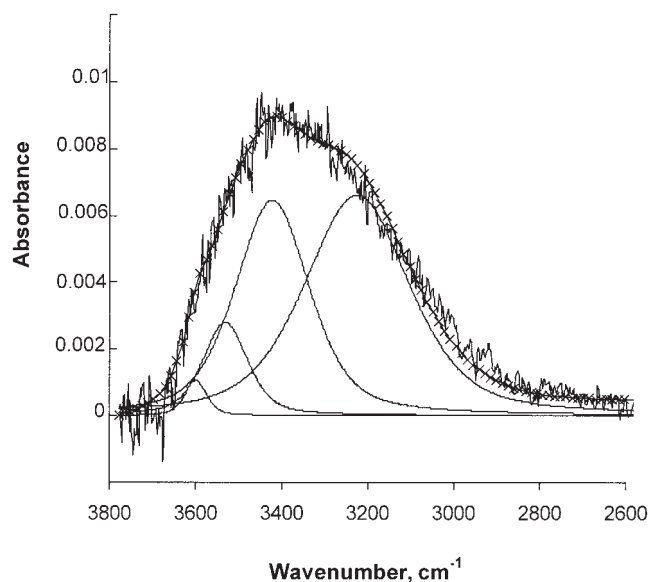


Figure 9 Band fitting results for water in AP-4; (-x-) fitted trace.

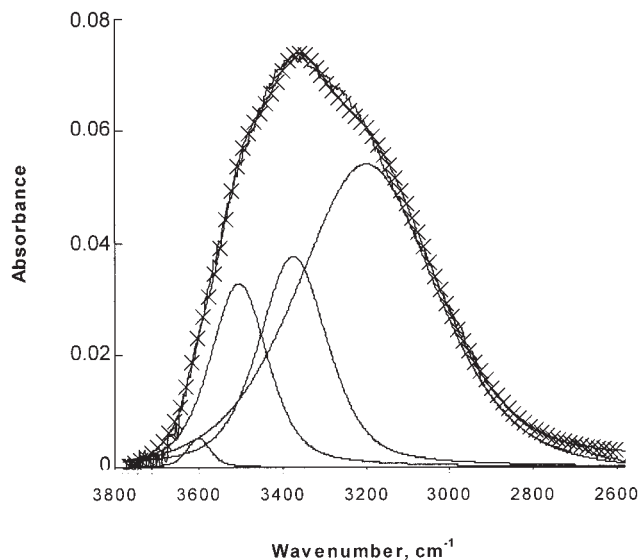


Figure 10 Band fitting results for water in AP-8; (-x-) fitted trace.

trimers, and small hydrogen-bonded clusters, respectively.¹⁹ Broad band 4 is attributable to a wide distribution of OH stretch vibration energies in hydrogen-bonded associated chains of water molecules.

From Table V, the following conclusions can be reached.

1. The spectral parameters of the non-hydrogen-bonded monomers, hydrogen-bonded dimers, and small hydrogen-bonded clusters (bands 1, 2, and 3) in AP show a general shift toward high frequency compared with those in bulk water. Moreover, the relative intensities of bands 1, 2, and 3 compared to those of component 4 were higher in the polymer than those in pure water. This shows that the amounts of $(\text{H}_2\text{O})_1$ and $(\text{H}_2\text{O})_{2,3}$ are relatively larger than water clusters in the polymer than in pure water. Because the absorptivity of the OH oscillators in non-hydrogen-bonded and poorly hydrogen-bonded water molecules is much smaller than that of fully hydrogen-bonded water,²⁰ the actual proportion of bands 1 and 2 relative to bands 3 and 4 is higher than indicated in Tables IV and V.
2. A similar although less pronounced trend was also observed with the 4.6 wt % titania filled hybrid (AP-2) where component bands 1 and 2 are more intense than in bulk water, relative to other bands.
3. Comparing the state of water in hybrids, it appears that the positions of bands 3 and 4 shift to lower wavenumbers with increasing titania content. In particular, the position of band 4 decreased from 3264 cm^{-1} for AP-2 to 3226 , 3225 , and 3199 cm^{-1} for AP-4, AP-6, and AP-8. respec-

TABLE IV
Band Parameters for Bulk Water (302 K)

Peak	Position (cm ⁻¹)		FWHM (cm ⁻¹)		Area (cm ⁻¹) This work	Rel. %	
	This work ^a	Ref. 18 ^b	This work	Ref. 18 ^b		This work	Ref. 18
1	3610	3613	82	77	3.4	2.7	1.8
2	3526	3526	134	140	11.8	9.5	7.5
3	3408	3395	197	216	45.0	36.3	36.4
4	3258	3224	272	263	63.9	51.5	54.3

FWHM, full width at half-maximum.

^a $T = 302$ K.

^b $T = 293$ K.

tively Simultaneously, the respective intensities of bands 1 and 4 decrease and increase with an increase in TiO₂ content.

Point 3 clearly shows that the environment of water in hybrids is different from that in a polymer matrix. The inorganic network with Ti—O—Ti groups (hydrogen-bond acceptors), residual Ti—OH groups (hydrogen-bond donors), and *in situ* generated hydrophilic sites likely interacts with water molecules through stronger hydrogen bondings than the acrylic polymer. Apart from a change in the chemical nature of the water environment, the titania network in hybrids induces an increase in the cluster size of water molecules and a broader distribution of hydrogen-stretch vibrations (larger line widths compared to the polymer film). On this subject, it is noteworthy that the state of water in the high titania filled hybrids (notably AP-6) approaches that of bulk water.

TABLE V
Band Parameters for Water at 302 K in Wet Films

Sample	Peak	Position (cm ⁻¹)	FWHM (cm ⁻¹)	Area (cm ⁻¹)	Rel. %
AP	1	3619	88	0.29	11.6
	2	3535	129	0.37	14.8
	3	3435	195	1.22	48.8
	4	3243	231	0.62	24.8
AP-2	1	3600	60	0.12	4.7
	2	3527	145	0.65	25.7
	3	3416	181	0.63	24.9
	4	3264	289	1.13	44.7
AP-4	1	3600	60	0.08	1.8
	2	3531	123	0.43	9.7
	3	3422	204	1.61	36.3
	4	3226	290	2.31	52.1
AP-6	1	3600	81	0.24	1.6
	2	3513	159	3.24	21.9
	3	3394	173	3.72	25.1
	4	3225	290	7.62	51.4
AP-8	1	3601	67	0.44	1.0
	2	3505	161	6.5	15.4
	3	3374	194	9.00	21.3
	4	3199	400	26.28	62.2

CONCLUSIONS

The water absorption characteristics of P(MMA-*co*-BMA-*co*-MA)/TiO₂ hybrids containing up to 16.3 wt % TiO₂ were investigated using the classical gravimetric method, FTIR spectroscopy, and TGA measurements, the two latter techniques being more relevant to clarify the structure of water in the composites. Although being somewhat speculative, we can try to make a connection between the gravimetric sorption results and the state of water revealed by TGA and FTIR spectroscopy. The following conclusions can be drawn.

The higher solubility of water in hybrids was related to the presence of additional hydrophilic sites carried by the titanium atoms either initially present in the dried hybrid or generated *in situ* (hydrolysis of carboxylate and butoxy ligands) during the absorption process. From the TGA and FTIR results it appears that the interactions between water and these hydrophilic sites is stronger and wider than with chemical groups from the polymer. This partly explains why the rate of water penetration is slowed down in hybrids compared to the polymer.

The negative effect of the *in situ* hydrolysis that brings a chemically driven force for water absorption becomes even more pronounced as it notably induces a breakage of crosslinks between the polymer and the inorganic phase and therefore a regain of mobility and available free space (diffusion coefficient increases when TiO₂ content goes up from 4.6 to 16.3 wt %). Interestingly, the FTIR spectroscopy results show that the water molecule clusters tend to increase in size for the highest filled hybrids.

To summarize, the water uptake characteristics in P(MMA-*co*-BMA-*co*-MA)/TiO₂ hybrids is mainly governed by the relative extent of two different effects. First, the inorganic network, being more dense, less mobile than the matrix polymer chain, and crosslinked to the polymer, exerts a positive effect on the water absorption characteristics (giving both lower solubility and slower diffusion). Second, the inorganic clusters bring additional hydrophilic sites either initially

present or generated after hydrolysis of coordinative bonds, thus activating the infiltration of additional water (i.e., increase in solubility). The influence of the latter phenomenon on D is hardly predictable because it suffers from two opposite effects (stronger interactions decrease D whereas hydrolytic breaking of crosslinks increase D).

The organic/inorganic hybrid with 4.6 wt % TiO₂ results in the best balance of properties with a far lower diffusion coefficient, nearly the same amount of water absorbed at saturation compared to the polymer matrix, and fairly good hydrolytic stability (insignificant amounts of released material). Moreover, it is noteworthy that a mild steel substrate coated with a 40 μm thick coating of the lowest filled Ti hybrid (AP-2) still did not reveal any corrosion spots after 5 months of immersion in a NaCl (3%) solution whereas the metals coated with the other coatings (acrylic polymer and highest filled hybrids) were severely attacked. Thus, for AP-2, the slightly higher hydrophilic character is not so harmful to the anticorrosive protection properties because it is largely balanced by the slower sorption rate and better adherence to the substrate.

The authors thank Egide for its financial support.

APPENDIX A

Relation between TGA results and actual water uptake

Let us consider a film with an initial weight m_0 (mg) that contains x (mg) residual volatiles. Let y (mg) be the water absorbed by the film after a time t (h) of immersion. The actual water uptake is

$$\phi(\%) = 100y/m_0 \quad (\text{A.1})$$

and

$$\text{TGA}_{0h} = 100x/m_0 \quad (\text{A.2})$$

where TGA_{0h} is the weight loss (%) obtained by TGA on the nonimmersed film. Consider now the two borderline cases. The *first case* is the total release of residual volatiles during immersion

$$\text{TGA}_{th} = \frac{100y}{m_0 - x + y} \quad (\text{A.3})$$

where TGA_{th} is the weight loss (%) obtained by TGA on the film immersed for t hours in water. Substituting eq. (A.2) in eq. (A.3) and then rearranging, we get

$$\phi(\%) = \frac{\text{TGA}_{th}(100 - \text{TGA}_{0h})}{100 - \text{TGA}_{th}} \quad (\text{A.4})$$

which is the *second case*, no release of volatiles.

Based on this assumption,

$$\text{TGA}_{th} = \frac{100(y + x)}{m_0 + y} \quad (\text{A.5})$$

Substituting eq. (A.2) in eq. (A.5) and then rearranging, we get

$$\phi(\%) = 100 \frac{(\text{TGA}_{th} - \text{TGA}_{0h})}{100 - \text{TGA}_{th}} \quad (\text{A.6})$$

References

1. Mark, J. E.; Lee, C. Y.-C.; Bianconi, P. A., Eds. Hybrid Organic-Inorganic Composites; ACS Symposium Series 585; American Chemical Society: Washington, DC, 1995.
2. Schubert, U. Chem Mater 2001, 13, 3487.
3. Landry, C. J. T.; Coltrain, B. K.; Brady, B. K. Polymer 1992, 33, 1486.
4. Perrin, F. X.; Nguyen, V. N.; Vernet, J. L. Polym Int 2002, 51, 1013.
5. Perrin, F. X.; Nguyen, V. N.; Vernet, J. L. Polymer 2002, 43, 6159.
6. Hinton, B. R. W. Metal Finish 1991, 89, 15.
7. Monte, J. S.; Sugerman, G. ACS Dev Org Coat Plast Chem 1980, 43, 158.
8. Stoye, D.; Freitag, W. Resins for Coatings—Chemistry, Properties and Applications; Hanser: Munich, 1996.
9. Funke, W. Prog Org Coat 1996, 28, 3.
10. Ahmad, Z.; Sarwar, M. I.; Wang, S.; Mark, J. E. Polymer 1997, 38, 4523.
11. Ahmad, Z.; Wang, S.; Mark, J. E. In Hybrid Organic-Inorganic Composites; Mark, J. E.; Lee, C. Y.-C.; Bianconi, P. A., Eds.; ACS Symposium Series 585; American Chemical Society: Washington, DC, 1995; p 291.
12. Lu, Z.; Liu, G.; Duncan, S. J Membr Sci 2003, 221, 113.
13. Shantali, T. A.; Karpova, I. L.; Dragan, K. S.; Privalko, E. G.; Privalko, V. P. Sci Technol Adv Mater 2003, 4, 115.
14. Perrin, F. X.; Nguyen, V. N.; Vernet, J. L. J Sol-Gel Sci Technol 2003, 28, 205.
15. Crank, J. The Mathematics of Diffusion; Oxford University Press: New York, 1975.
16. Wiggins, P. M. Prog Polym Sci 1988, 13, 1.
17. Sutandar, P.; Ahn, D. J.; Franses, E. I. Macromolecules 1994, 27, 7316.
18. Sammon, Ch.; Mura, C.; Yarwood, J.; Everall, N.; Swart, R.; Hodge, D. J Phys Chem B 1998, 102, 3402.
19. Jain, K. J.; Varshney, M.; Maitra, A. J Phys Chem 1989, 93, 7409.
20. Walrafen, G. E. In Water, a Comprehensive Treatise: The Physics and Physical Chemistry of Water; Franks, F., Ed.; Plenum: New York, 1972; Vol. 1, p 202.